

# Heavy-ion double-charge-exchange and its relation to neutrinoless double- $\beta$ decay

Elena Santopinto

INFN-Genova

for the NUMEN collaboration

Based on

Santopinto, Garcia Tecocoatzi, Magaña Vsevolodovna, Ferretti, *PRC***98**,061601(R),2018

·

**12<sup>th</sup> Matrix Elements for the Double beta decay Experiments**

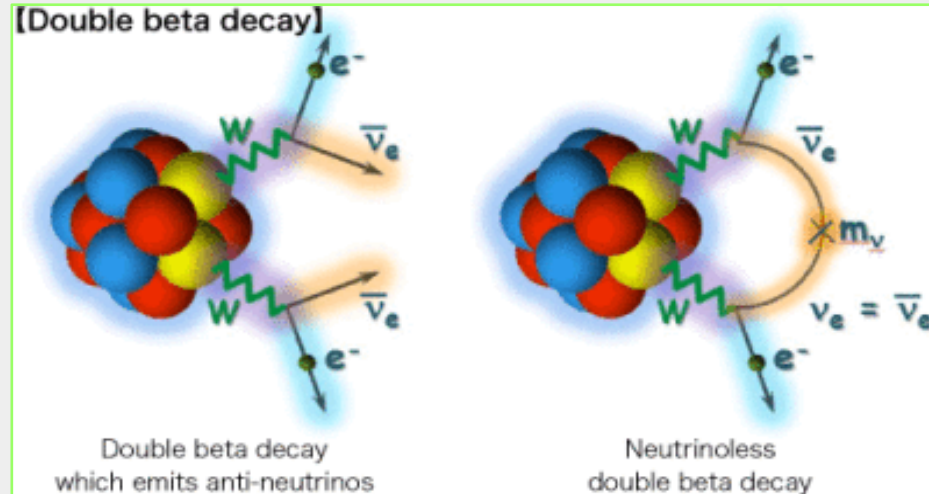
Prague 27-31 May, 2019

# Table of Content

- Double beta decay
- Double charge exchange
- Effective potential for DCE
- DCE- cross-section
- DCE matrix elements
- Results
- Conclusions and future work



# Double beta decay



Double beta decay with neutrinos (observed).

These decays are usually ground state to ground state transitions.

Quenching of  $g_A$

Neutrinoless double beta decay

Lepton number conservation is broken.

Is the neutrino a Majorana particle?

Physics beyond Standard model

## Neutrinoless double beta decay

$$\left[ T_{1/2}^{0\nu} (0^+ \rightarrow 0^+) \right]^{-1} = G^{0\nu}(E_0, Z) |M^{0\nu}|^2 \langle m_{\nu_e} \rangle^2$$

$0\nu\beta\beta$  Nuclear Matrix Element

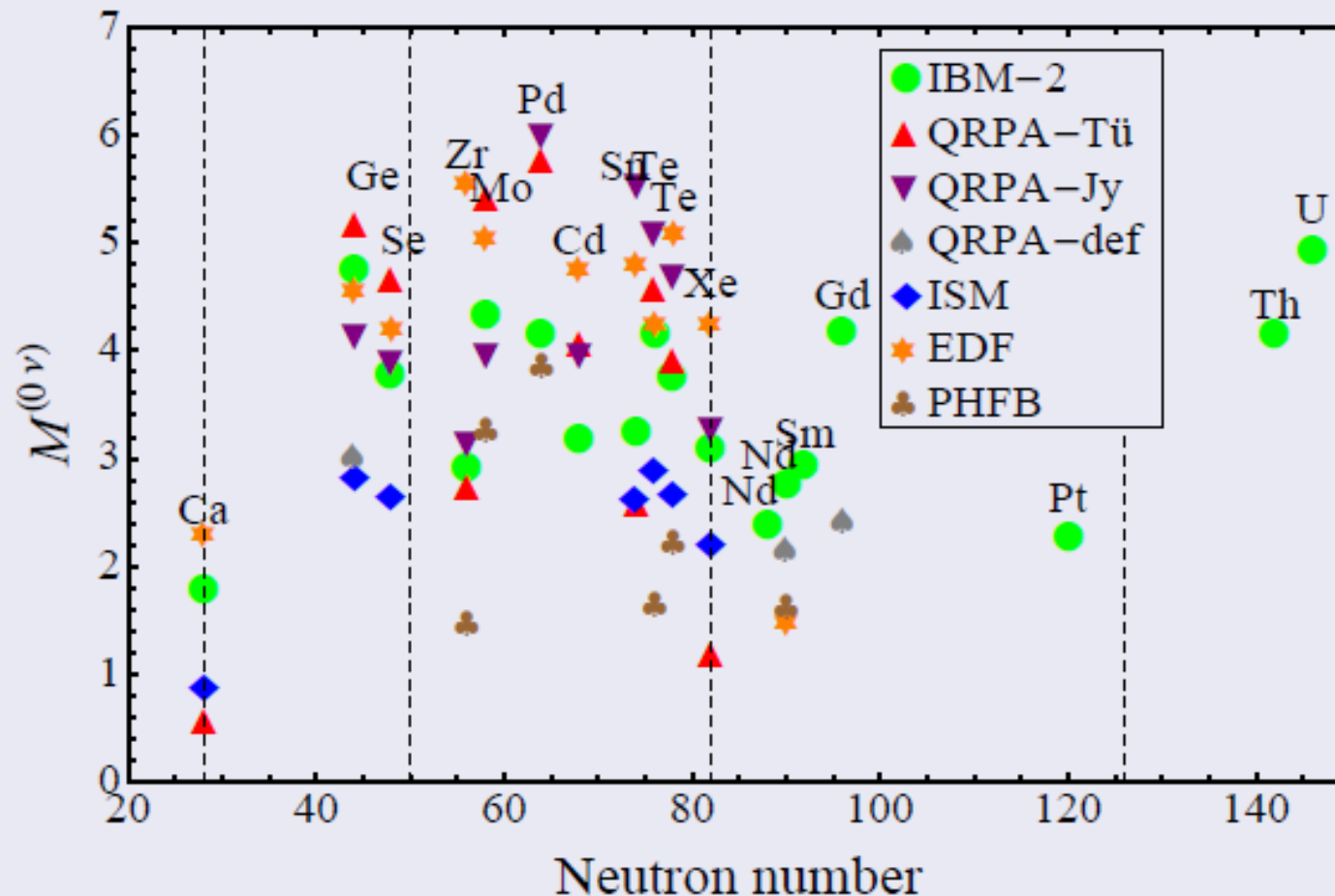
$$|M^{0\nu}|^2 = \left| \langle \Psi_f | \hat{O}_\varepsilon^{\beta\beta 0\nu} | \Psi_i \rangle \right|^2$$

phase space factor and a factor that depends on the masses and the mixing coefficients of the neutrinos

# Nuclear matrix elements for Neutrinoless double beta decay

tensions in NME calculations

$$M^{(0\nu)} = M_{GT}^{(0\nu)} - \left(\frac{g_V}{g_A}\right)^2 M_F^{(0\nu)} + M_T^{(0\nu)}$$



# Double Charge Exchange Experiment

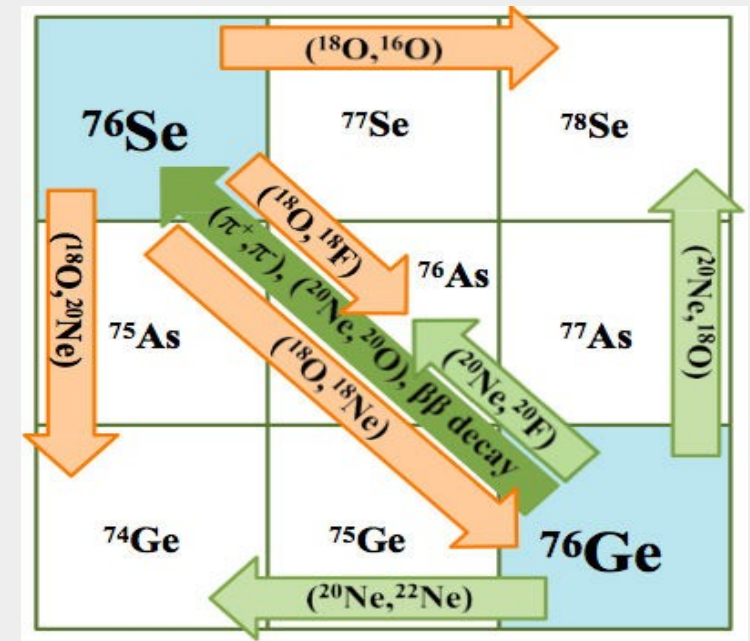
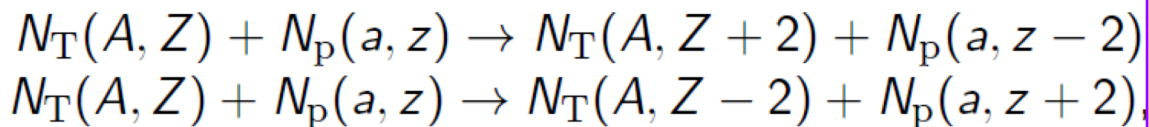


- Candidates isotopes:  $^{48}\text{Ca}$ ,  $^{82}\text{Se}$ ,  $^{100}\text{Mo}$ ,  $^{124}\text{Sn}$ ,  $^{128}\text{Te}$ ,  $^{130}\text{Te}$ ,  $^{136}\text{Xe}$ ,  $^{148}\text{Nd}$ ,  $^{150}\text{Nd}$ ,  $^{154}\text{Sm}$ ,  $^{160}\text{Gd}$ ,  $^{198}\text{Pt}$ .

# Heavy Ion Double Charge Exchange

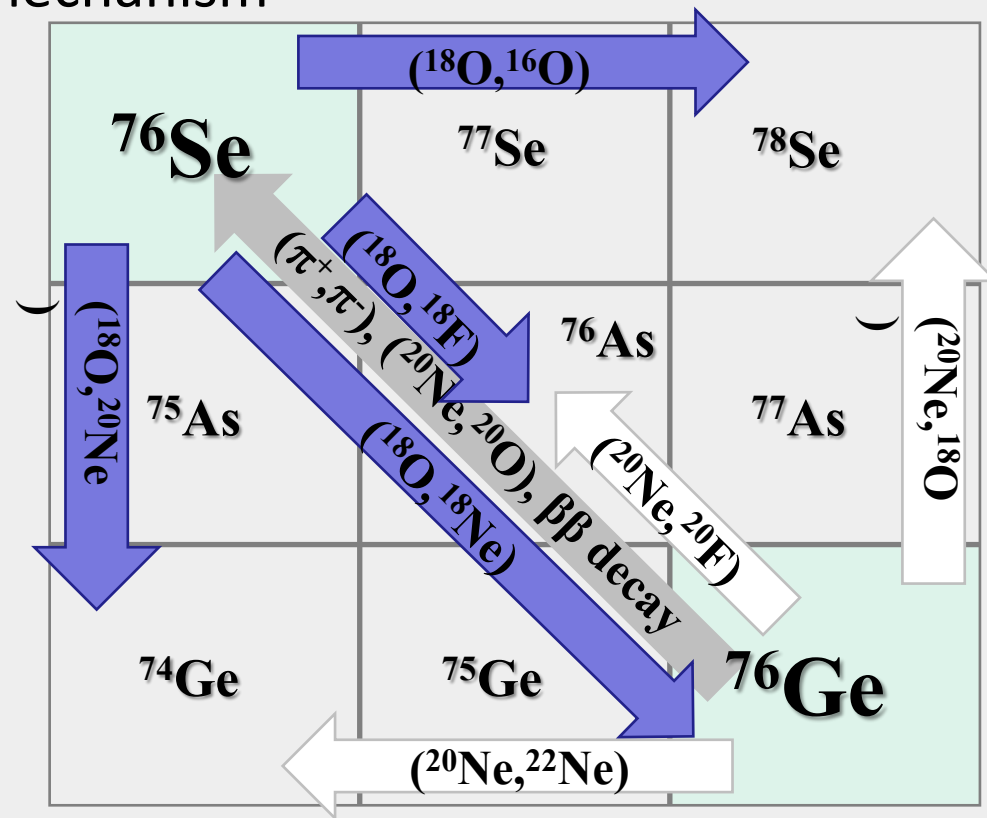
In heavy-ion DCE reactions two protons (neutrons) are converted into two neutrons (protons) in the target, and two neutrons (protons) are converted into two protons (neutrons) in the projectile, while the mass number of the target,  $A$ , and of the projectile,  $a$ , both remain unchanged.

So in heavy ion DCE reactions,  
we study the following reactions  
with the exchange of two units of charge  
between the target and projectile



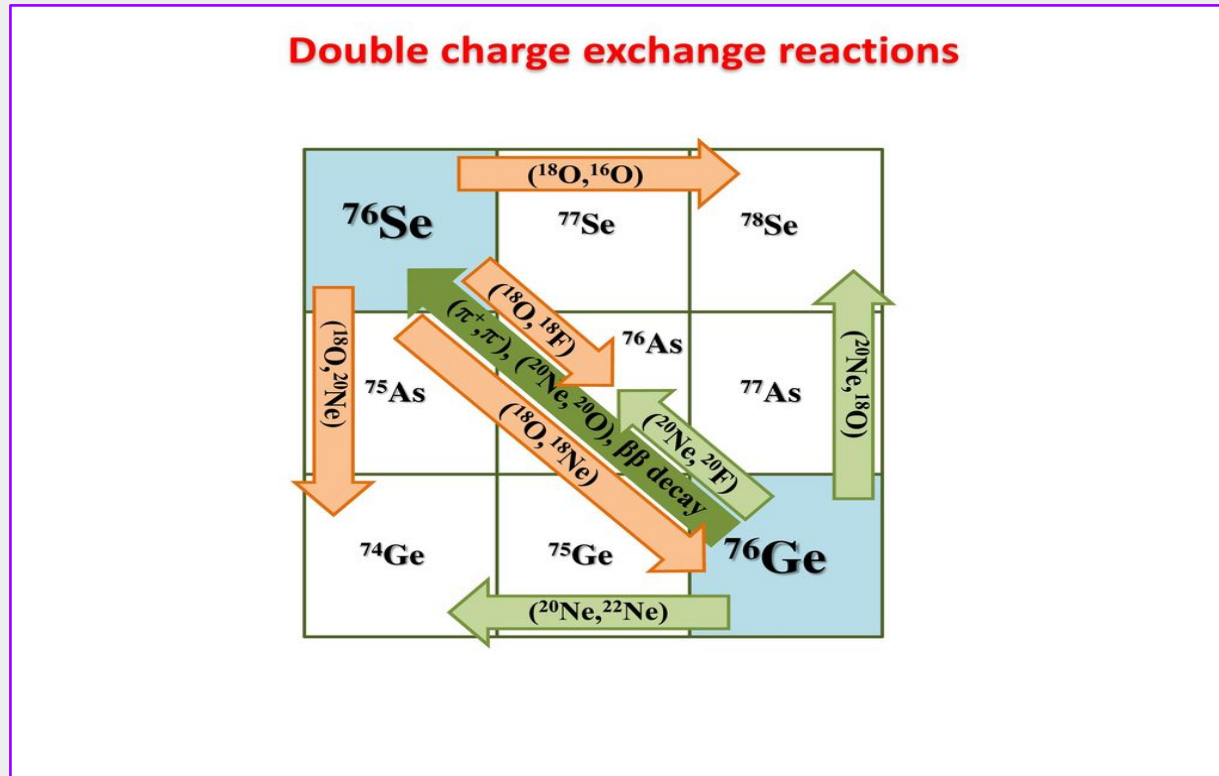
## Heavy-Ion Double Charge-Exchange (DCE)

- ✓ Induced by strong interaction
- ✓ Meson exchange mechanism
- ✓ Sequential nucleon transfer mechanism





# Heavy ion DCE vs two-proton and two-neutron transfer



We have shown that these competing processes are far from saturating the total detected experimental cross-section, NUMEN collaboration, Eur. Phys. J. A (2018) 54: 72

The nucleon-nucleon charge-exchange effective potential we consider,

$$V_{\text{CE}}(\vec{q}) = V_{\text{OPE}}(\vec{q}) + V_{\text{ZR}} ,$$

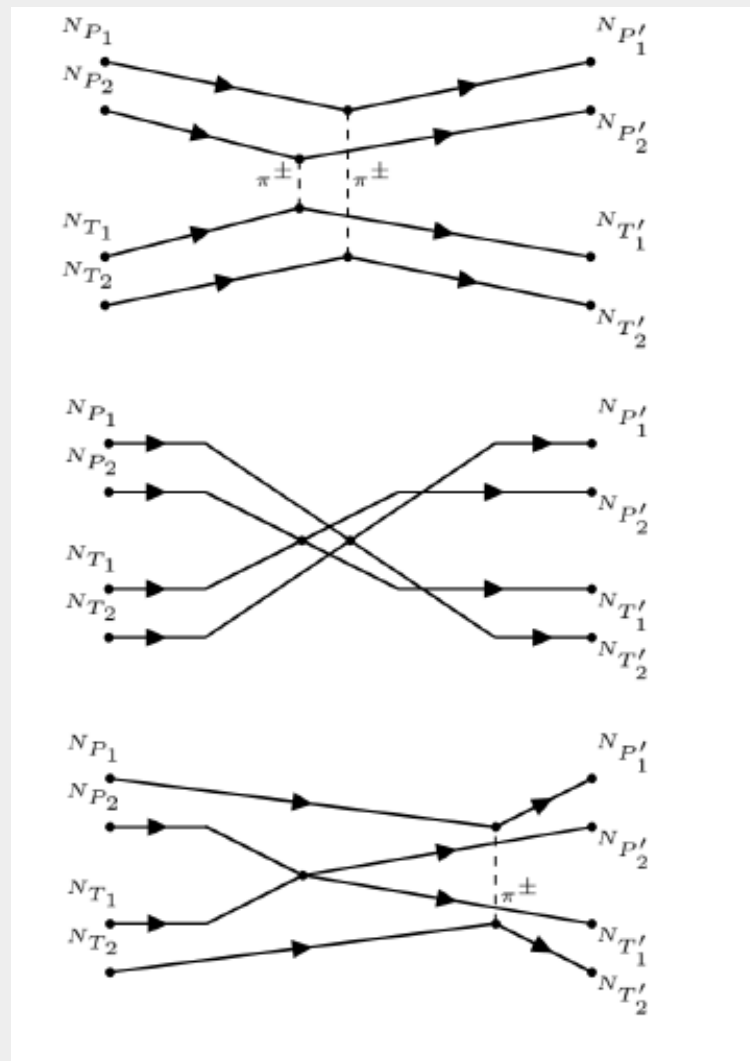
is the sum of a long- and medium-range one-pion exchange (OPE) and an effective zero-range (ZR) contact interaction, as from

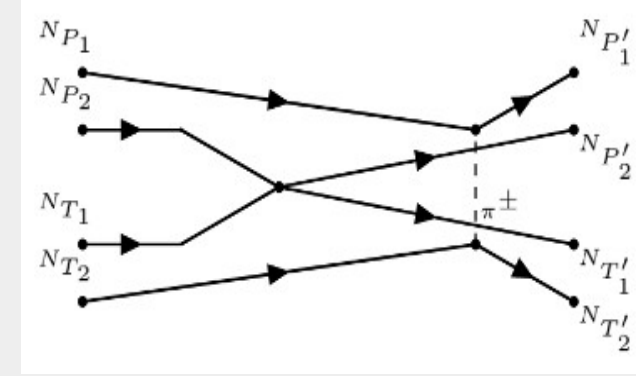
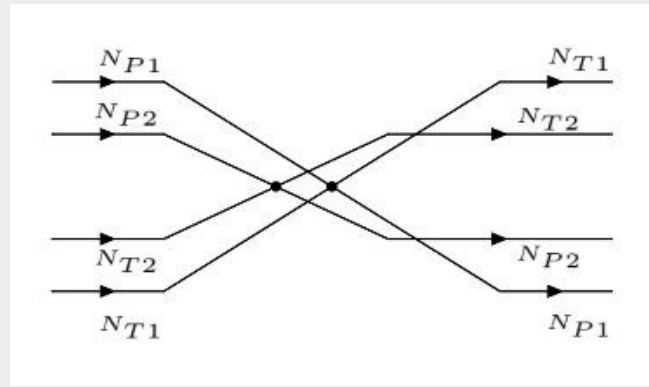
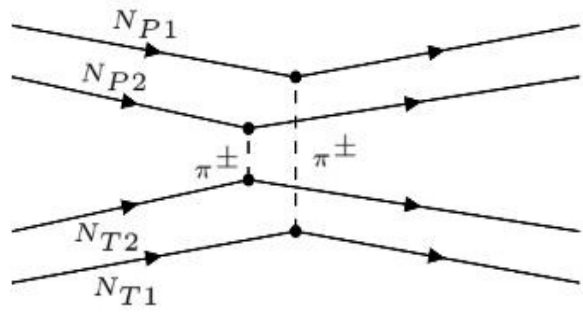
G. F. Bertsch and H. Esbensen, Rep. Prog. Phys. 50, 607 (1987).

The latter, due to many body correlations, is written in coordinate space as follows

$$V_{\text{ZR}}(\vec{r}) = [c_{\text{T}}(\vec{\tau}_1 \cdot \vec{\tau}_2) + c_{\text{GT}}(\vec{\sigma}_1 \cdot \vec{\sigma}_2)(\vec{\tau}_1 \cdot \vec{\tau}_2)] \delta^3(\vec{r}) ,$$

The OPE and ZR interactions provide the expressions for the vertices which we need in the computation of the diagrams in Fig.





We derived the DCE effective potential (in closure approximation):

$$\begin{aligned}
 V^{\text{DCE}}(\vec{q}_1, \vec{q}_2) = & \frac{4}{3} \left( \frac{f_\pi}{m_\pi} \right)^4 \left( \frac{(\vec{\sigma}_{P1} \cdot \vec{q}_1)(\vec{\sigma}_{T1} \cdot \vec{q}_1)}{\omega_1(\omega_1 + \bar{E}_P)} \vec{v}_{P1} \cdot \vec{v}_{T1} \right) \left( \frac{(\vec{\sigma}_{P2} \cdot \vec{q}_2)(\vec{\sigma}_{T2} \cdot \vec{q}_2)}{\omega_2(\omega_2 + \bar{E}_P)(\omega_2 + \bar{E}_T)} \vec{v}_{P2} \cdot \vec{v}_{T2} \right) \\
 & + 2 \left[ \frac{c_T^2}{\bar{E}_P^F + \bar{E}_T^F} + \frac{c_{GT}^2 (\vec{\sigma}_{P1} \cdot \vec{\sigma}_{T1})(\vec{\sigma}_{P2} \cdot \vec{\sigma}_{T2})}{\bar{E}_P^{GT} + \bar{E}_T^{GT}} + \frac{c_{TCGT} (\vec{\sigma}_{P2} \cdot \vec{\sigma}_{T2})}{\bar{E}_P^{GT} + \bar{E}_T^F} + \frac{c_{TCGT} (\vec{\sigma}_{P1} \cdot \vec{\sigma}_{T1})}{\bar{E}_P^F + \bar{E}_T^{GT}} \right] (\vec{v}_{P1} \cdot \vec{v}_{T1})(\vec{v}_{P2} \cdot \vec{v}_{T2}) \\
 & + \left[ \left( \frac{f_\pi}{m_\pi} \right)^2 \left( \frac{(\vec{\sigma}_{P1} \cdot \vec{q}_1)(\vec{\sigma}_{T1} \cdot \vec{q}_1)}{\omega_1(\omega_1 + \bar{E}_P)(\omega_1 + \bar{E}_T)} \vec{v}_{P1} \cdot \vec{v}_{T1} \right) [c_T(\vec{v}_{P2} \cdot \vec{v}_{T2}) + c_{GT}(\vec{\sigma}_{P2} \cdot \vec{\sigma}_{T2})(\vec{v}_{P2} \cdot \vec{v}_{T2})] + 1 \leftrightarrow 2 \right]. \quad (3)
 \end{aligned}$$

and in the low momentum transfer the DCE potential can be simply written as:

$$V^{\text{DCE}} \xrightarrow{\vec{Q} \rightarrow 0} 2 \left[ \frac{c_T^2}{\bar{E}_P^F + \bar{E}_T^F} + \frac{c_{GT}^2 (\vec{\sigma}_{P1} \cdot \vec{\sigma}_{T1})(\vec{\sigma}_{P2} \cdot \vec{\sigma}_{T2})}{\bar{E}_P^{GT} + \bar{E}_T^{GT}} + \frac{c_{TCGT} (\vec{\sigma}_{P2} \cdot \vec{\sigma}_{T2})}{\bar{E}_P^{GT} + \bar{E}_T^F} + \frac{c_{TCGT} (\vec{\sigma}_{P1} \cdot \vec{\sigma}_{T1})}{\bar{E}_P^F + \bar{E}_T^{GT}} \right] (\vec{v}_{P1} \cdot \vec{v}_{T1})(\vec{v}_{P2} \cdot \vec{v}_{T2})$$

since it is dominated by the contact interaction.

# Differential cross-section

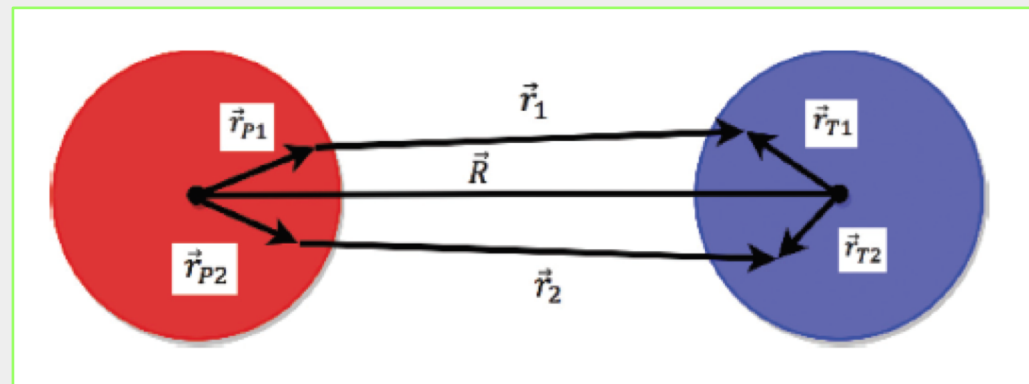
PHYSICAL REVIEW C 98, 061601(R) (2018)

- We apply our formalism for describing DCE cross section in the Eikonal approximation

$$\frac{d\sigma}{d\Omega} = \frac{k}{k'} \left( \frac{\mu}{4\pi^2 \hbar^2} \right)^2 |T_{if}|^2$$

$$\begin{aligned} T_{if} &= \langle \Psi_{k'}^- \Phi_f | V | \Psi_k^+ \Phi_i \rangle \\ &= \frac{1}{(2\pi)^{3/2}} \int d\vec{R} e^{i(\chi(b) - \vec{Q} \cdot \vec{R})} M_{if}(\vec{m}) \end{aligned}$$

$$\Psi_{k'}^-(\vec{R}) \Psi_k^+(\vec{R}) = \frac{1}{(2\pi)^{3/2}} e^{i(\chi(b) - \vec{Q} \cdot \vec{R})}$$



# Differential cross-section in low-momentum-transfer limit

Santopinto et al., PRC98, 061601(R) (2018)

- The effective DCE potential for small angles

$$V^{\text{DCE}} \xrightarrow{\bar{Q} \rightarrow 0} 2 \left[ \frac{c_T^2}{\bar{E}_P^F + \bar{E}_T^F} + \frac{c_{\text{GT}}^2 (\vec{\sigma}_{P1} \cdot \vec{\sigma}_{T1}) (\vec{\sigma}_{P2} \cdot \vec{\sigma}_{T2})}{\bar{E}_P^{\text{GT}} + \bar{E}_T^{\text{GT}}} + \frac{c_T c_{\text{GT}} (\vec{\sigma}_{P2} \cdot \vec{\sigma}_{T2})}{\bar{E}_P^{\text{GT}} + \bar{E}_T^F} + \frac{c_T c_{\text{GT}} (\vec{\sigma}_{P1} \cdot \vec{\sigma}_{T1})}{\bar{E}_P^F + \bar{E}_T^{\text{GT}}} \right] (\vec{\tau}_{P1} \cdot \vec{\tau}_{T1}) (\vec{\tau}_{P2} \cdot \vec{\tau}_{T2})$$

$$M_{\text{if}}(\mathbf{m}) = \langle \Phi_f | V^{\text{DCE}} | \Phi_i \rangle ,$$

The transition amplitude in the low-momentum-transfer limit is

$$M_{\text{if}}(\mathbf{m}) \xrightarrow{\bar{Q} \rightarrow 0} 6 \sum_J \begin{Bmatrix} 1 & 1 & J \\ 1 & 1 & J \\ 0 & 0 & 0 \end{Bmatrix} \langle \phi_f^{T1} \phi_f^{P1} \phi_f^{T2} \phi_f^{P2} | \left\{ \frac{c_{\text{GT}}^2 (2J+1)}{\bar{E}_P^{\text{GT}} + \bar{E}_T^{\text{GT}}} [(\vec{\sigma}_{P1} \times \vec{\sigma}_{P2})^{(J)} (\vec{\sigma}_{T1} \times \vec{\sigma}_{T2})^{(J)}]^{(0)} \right. \\ \left. + \frac{c_T^2 \delta_{J,0}}{\bar{E}_P^F + \bar{E}_T^F} + \sqrt{3} c_T c_{\text{GT}} \delta_{J,0} \left( \frac{(\vec{\sigma}_{P2} \times \vec{\sigma}_{T2})^{(0)}}{\bar{E}_P^{\text{GT}} + \bar{E}_T^F} + \frac{(\vec{\sigma}_{P1} \times \vec{\sigma}_{T1})^{(0)}}{\bar{E}_P^F + \bar{E}_T^{\text{GT}}} \right) \right\} (\tau_{T1}^+ \tau_{T2}^+ \tau_{P1}^- \tau_{P2}^-) | \phi_i^{T1} \phi_i^{P1} \phi_i^{T2} \phi_i^{P2} \rangle ,$$

If we study transitions 0+ ground state to 0+ ground state we can rewrite in a compact form

# Transition amplitude between ground states

PHYSICAL REVIEW C 98, 061601(R) (2018)

- The amplitude between ground states can be computed as follows

$$M_{\text{if}}(\mathbf{m}) \xrightarrow{\vec{Q} \rightarrow 0} 2 \left[ \left( \frac{\mathcal{M}_{T \rightarrow T'}^{\text{DGT}} \mathcal{M}_{P \rightarrow P'}^{\text{DGT}}}{\bar{E}_P^{\text{GT}} + \bar{E}_T^{\text{GT}}} \right) + \left( \frac{\mathcal{M}_{T \rightarrow T'}^{\text{DF}} \mathcal{M}_{P \rightarrow P'}^{\text{DF}}}{\bar{E}_P^{\text{F}} + \bar{E}_T^{\text{F}}} \right) \right],$$

$$\mathcal{M}_{A \rightarrow A'}^{\text{DGT}} = c_{\text{GT}} \langle \Phi_{J'}^{(A')} | \sum_{n, n'} [\vec{\sigma}_n \times \vec{\sigma}_{n'}]^{(0)} \vec{\tau}_n \vec{\tau}_{n'} | \Phi_J^{(A)} \rangle,$$

$$\mathcal{M}_{A \rightarrow A'}^{\text{DF}} = c_{\text{T}} \langle \Phi_{J'}^{(A')} | \sum_{n, n'} \vec{\tau}_n \vec{\tau}_{n'} | \Phi_J^{(A)} \rangle$$

$$\frac{d\sigma}{d\Omega} \xrightarrow{\vec{Q} \rightarrow \mathbf{0}} \frac{k}{k'} \left( \frac{\mu}{4\pi^2 \hbar^2} \right)^2 \left| 2F(\theta) \left( \frac{\mathcal{M}_{T \rightarrow T'}^{\text{DGT}} \mathcal{M}_{P \rightarrow P'}^{\text{DGT}}}{\bar{E}_p^{\text{GT}} + \bar{E}_t^{\text{GT}}} + \frac{\mathcal{M}_{T \rightarrow T'}^{\text{DF}} \mathcal{M}_{P \rightarrow P'}^{\text{DF}}}{\bar{E}_p^{\text{F}} + \bar{E}_t^{\text{F}}} \right) \right|^2$$

$$F(\theta) \xrightarrow{Q_z \rightarrow 0} 2\pi \int_{-\infty}^{\infty} dz \int_0^{\infty} db e^{-izQ_z} b J_0(kb \sin \theta) e^{i\chi(b)}$$

- The cross-section in the eikonal approximation and low-momentum transfer limit is given as follows

$$\frac{d\sigma}{d\Omega} \Big|_{[\vec{Q} \rightarrow 0]} \rightarrow \frac{k}{k'} \left( \frac{\mu}{4\pi^2 \hbar^2} \right)^2 \left| 2F(\theta) \left( \frac{\mathcal{M}_{T \rightarrow T'}^{\text{DGT}} \mathcal{M}_{P \rightarrow P'}^{\text{DGT}}}{\bar{E}_P^{\text{GT}} + \bar{E}_T^{\text{GT}}} + \frac{\mathcal{M}_{T \rightarrow T'}^{\text{DF}} \mathcal{M}_{P \rightarrow P'}^{\text{DF}}}{\bar{E}_P^{\text{F}} + \bar{E}_T^{\text{F}}} \right) \right|^2,$$

where  $\mu$  is the reduced mass of the target-projectile system and  $F(\theta)$  is the scattering angular distribution.



## DCE Nuclear Matrix Elements

DCE-Double-Gamow-Teller (DGT) and DCE-Double-Fermi (DF) matrix elements, respectively, for a given nuclear transition of the projectile/target ( $A = P, T$ ), defined as

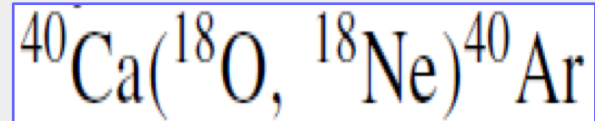
$$\mathcal{M}_{A \rightarrow A'}^{\text{DF}} = c_{\text{T}} \left\langle \Phi_{J'}^{(A')} \left| \sum_{n, n'} \tau_n^\dagger \tau_{n'}^\dagger \right| \Phi_J^{(A)} \right\rangle ,$$

and

$$\mathcal{M}_{A \rightarrow A'}^{\text{DGT}} = c_{\text{GT}} \left\langle \Phi_{J'}^{(A')} \left| \sum_{n, n'} [\vec{\sigma}_n \times \vec{\sigma}_{n'}]^{(0)} \tau_n^\dagger \tau_{n'}^\dagger \right| \Phi_J^{(A)} \right\rangle ,$$

where the sum is over the nucleons ( $n, n'$ ) involved in the process.

# Theoretical description of



- We describe the reaction for small angles

Reaction $^{18}\text{O} \rightarrow ^{18}\text{Ne}$	$\mathcal{M}_{\text{DCE}}^{\text{P,DGT}}$ 0.86	$\mathcal{M}_{\text{DCE}}^{\text{P,DF}}$ 0.35
Reaction $^{40}\text{Ca} \rightarrow ^{40}\text{Ar}$	$\mathcal{M}_{\text{DCE}}^{\text{T,DGT}}$ 0.42	$\mathcal{M}_{\text{DCE}}^{\text{T,DF}}$ 0.17

- Our cross-section is  $8.9 \mu\text{b}/\text{sr}$  which is in good agreement with the experimental data Eur. Phys. J. A **51**, 145 (2015).

## Results for $^{40}\text{Ca}(^{18}\text{O}, ^{18}\text{Ne})^{40}\text{Ar}$

We computed the  $^{40}\text{Ca}(^{18}\text{O}, ^{18}\text{Ne})^{40}\text{Ar}$  DCE cross-section at  $\theta = 0$ .

We obtained a value of  $8.9\mu\text{b}/\text{sr}$  inside the experimental range,  $(8.0 - 10.5)\mu\text{b}/\text{sr}$  (Eur. Phys J.A (2015) 51 145).

# Calculation of DGT- DF NME's for $0\nu\beta\beta$ decay candidate with microscopic IBM2

- We compute DGT-DF NME in microscopic IBM, PRC 98, 061601(R) (2018)

Reaction	$\mathcal{M}_{DCE}^{T,DGT}$	$\mathcal{M}_{DCE}^{T,DF}$	$\mathcal{M}_{0\nu\beta\beta}^{T,DGT}$	$\mathcal{M}_{0\nu\beta\beta}^{T,DF}$	$\mathcal{M}_{0\nu\beta\beta}^{TOT}$
$^{116}\text{Cd} \rightarrow ^{116}\text{Sn}$	0.20	0.05	0.21	-0.02	0.25
$^{82}\text{Se} \rightarrow ^{82}\text{Kr}$	0.28	0.08	0.31	-0.21	0.50
$^{128}\text{Te} \rightarrow ^{128}\text{Xe}$	0.27	0.07	0.28	-0.16	0.43
$^{76}\text{Ge} \rightarrow ^{76}\text{Se}$	0.34	0.10	0.40	-0.25	0.63

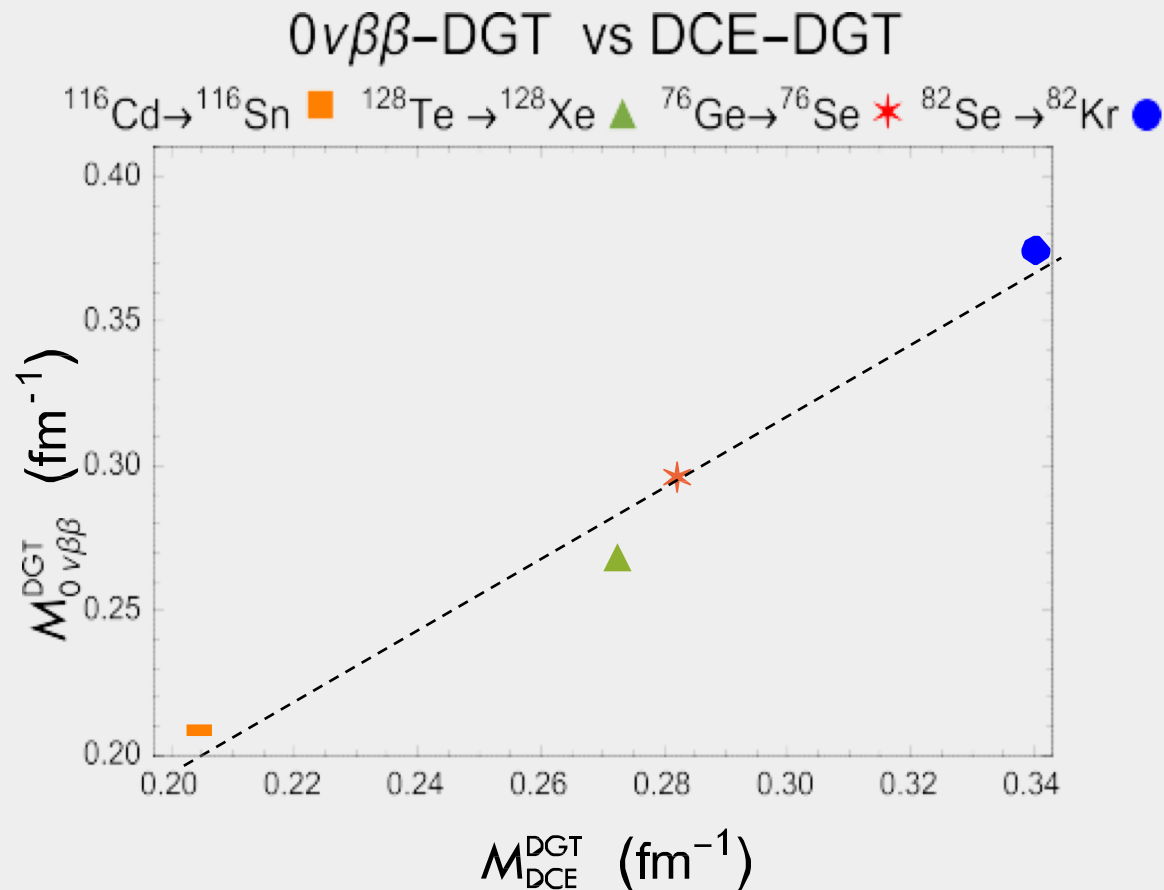
The matrix elements are in fm<sup>-1</sup>. The value of the constants are  $c_t = 151 \text{ MeV fm}^3$  and  $c_{gt} = 217 \text{ MeV fm}^3$  from G.F Bertsch et al., Rep. Prog. Phys. 50 607 (1987). **We can observe that the dominant contribution is the Double Gamow-Teller.**

- The  $0\nu\beta\beta$  NME's were taken from Ref. Phys. Rev. C 87, 014315, 2013, with  $g_A=1$ , using

$$\mathcal{M}_{0\nu\beta\beta}^{TOT} = \mathcal{M}_{0\nu\beta\beta}^{GT} - \left(\frac{g_V}{g_A}\right)^2 \mathcal{M}_{0\nu\beta\beta}^F + \mathcal{M}_{0\nu\beta\beta}^T$$

# Linear Correlation of DGT NME's

PHYSICAL REVIEW C 98, 061601(R) (2018)

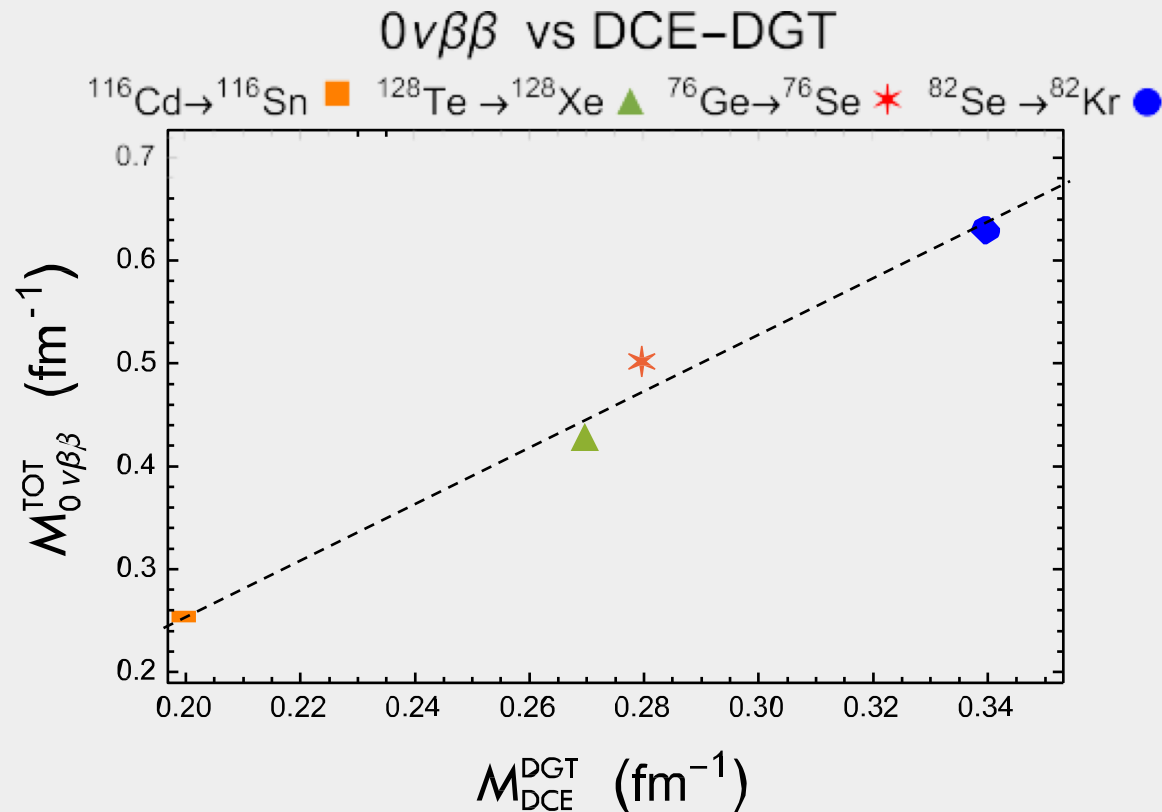


21 / 17see

See also N. Shimitzu Phys. Rev. Lett 120 142502 (2018).

# Linear Correlation

There is linear correlation between total nuclear matrix elements of  $0\nu\beta\beta$ -decay and Double Gamow Teller in DCX too.



# The linear correlation

We investigate a linear correlation between  $0\nu\beta\beta$  and DCE NME's that was found in Phys. Rev. Lett. 120, 142502 (2018) for DGT transitions, and we confirm

$$B(\text{DGT}^\pm; \lambda; i \rightarrow f) = \frac{1}{2J_i + 1} |\langle f || \mathcal{O}_\pm^{(\lambda)} || i \rangle|^2,$$

However, there is a strong dependence on  $g_A$

$$\mathcal{M}_{0\nu\beta\beta}^{\text{TOT}} = \mathcal{M}_{0\nu\beta\beta}^{\text{GT}} - \left(\frac{g_V}{g_A}\right)^2 \mathcal{M}_{0\nu\beta\beta}^{\text{F}} + \mathcal{M}_{0\nu\beta\beta}^{\text{T}}$$

$$g_A = \begin{cases} 1.269, \\ 1, \\ 1.269 A^{-0.18}, \end{cases}$$

# Linear correlation

PHYSICAL REVIEW C 98, 061601(R) (2018)

- We find also a linear correlations between the Total NME's, but it depends on  $g_A$

$$\mathcal{M}_{0\nu\beta\beta}^{\text{TOT}} \Big|_{g_A=1} = -0.29 + 2.74 \mathcal{M}_{\text{DCE}}^{\text{T,DGT}}$$

$$\mathcal{M}_{0\nu\beta\beta}^{\text{TOT}} \Big|_{g_A=1.269 A^{-0.18}} = -0.78 + 5.84 \mathcal{M}_{\text{DCE}}^{\text{T,DGT}}$$

For the DGT-DCE we got

$$\mathcal{M}_{0\nu\beta\beta}^{\text{DGT}} = -0.07 + 1.36 \mathcal{M}_{\text{DCE}}^{\text{T,DGT}}$$



# Conclusions

- We derived, for the first time, an effective potential that describes the DCE reactions.
- For the first time, we demonstrated that the expression for the DCE-differential cross-section can be factorized in the DCE-NME's and the reaction part, in Eikonal approximation and very forward angles.
- For the first time, we identified a DGT and DF NME's at  $\theta=0$
- We observed a linear correlation between DGT-DCE and  $0\nu\beta\beta$  NME, but the total NME's depend on  $g_A$ . Which is in agreement with N. Shimitzu Phys. Rev. Lett 120 142502 (2018).
- In DCE, the DCE-DGT contribution is the dominant one.

# Conclusions and future work

- The DCE differential cross-section is dominated by contact interactions at  $\theta=0$ . The factorization plus the linear correlation open the possibility of placing constraints in  $0\nu\beta\beta$  NME, using future data by NUMEN.

## Future Work

- Calculate the differential cross-section for more angles.

Thank you for your attention